

General Disclaimer

One or more of the Following Statements may affect this Document

- This document has been reproduced from the best copy furnished by the organizational source. It is being released in the interest of making available as much information as possible.
- This document may contain data, which exceeds the sheet parameters. It was furnished in this condition by the organizational source and is the best copy available.
- This document may contain tone-on-tone or color graphs, charts and/or pictures, which have been reproduced in black and white.
- This document is paginated as submitted by the original source.
- Portions of this document are not fully legible due to the historical nature of some of the material. However, it is the best reproduction available from the original submission.

NASA TECHNICAL
MEMORANDUM

NASA TM X-73,201

NASA TM X-73 201

(NASA-TM-X-73201) DISCHARGE STABILIZATION
STUDIES OF CO LASER GAS MIXTURES IN
QUASI-STEADY SUPERSONIC FLOW (NASA) 28 p HC
A03/MF A01 CSCL 20E

N77-20428

G3/36

Unclas
21710

DISCHARGE STABILIZATION STUDIES OF CO LASER GAS
MIXTURES IN QUASI-STEADY SUPERSONIC FLOW

G. Srinivasan and J. A. Smith

Ames Research Center
Moffett Field, California 94035

October 1976

1. Report No. NASA TM X-73,201	2. Government Accession No.	3. Recipient's Catalog No.	
4. Title and Subtitle DISCHARGE STABILIZATION STUDIES OF CO LASER GAS MIXTURES IN QUASI-STEADY SUPERSONIC FLOW		5. Report Date	
		6. Performing Organization Code	
7. Author(s) G. Srinivasan* and J. A. Smith**		8. Performing Organization Report No. A-6897	
		10. Work Unit No. 506-25-32	
9. Performing Organization Name and Address Ames Research Center, NASA Moffett Field, Calif. 94035		11. Contract or Grant No.	
		13. Type of Report and Period Covered Technical Memorandum	
12. Sponsoring Agency Name and Address National Aeronautics and Space Administration Washington, D.C. 20546		14. Sponsoring Agency Code	
15. Supplementary Notes *National Research Council Postdoctoral Research Associate. **Permanent address: Gas Dynamics Laboratory, Forrestal Campus, Princeton University, Princeton, N.J. 08540.			
16. Abstract Experiments have been conducted to study the applicability of a double discharge stabilization scheme in conditions appropriate for high energy CO lasers in supersonic flows. A Ludwig tube impulse flow facility and a ballasted capacitor bank provided essentially steady flow and discharge conditions (d.c.) for times longer than ten electrode length-flow transit times. Steady, arc-free, volume discharges have been produced in a Mach 3 test cavity using an auxiliary discharge to stabilize the main discharge in N ₂ and He/CO mixtures. A significant result is the lack of observed plasma E/N changes in response to auxiliary discharge current changes. Also, where glow discharges were obtained, the energy loading achieved was very much less than the threshold level required for laser operation.			
17. Key Words (Suggested by Author(s)) Lasers Electric discharge Supersonic flow Carbon monoxide		18. Distribution Statement Unlimited STAR Category - 36	
19. Security Classif. (of this report) Unclassified	20. Security Classif. (of this page) Unclassified	21. No. of Pages 27	22. Price* \$3.75

DISCHARGE STABILIZATION STUDIES OF CO LASER GAS
MIXTURES IN QUASI-STEADY SUPERSONIC FLOW

G. Srinivasan* and J. A. Smith**

Ames Research Center

SUMMARY

Experiments have been conducted to study the applicability of a double discharge stabilization scheme in conditions appropriate for high energy CO lasers in supersonic flows. A Ludwig tube impulse flow facility and a ballasted capacitor bank provided essentially steady flow and discharge conditions (d.c.) for times longer than ten electrode length-flow transit times. Steady, arc-free, volume discharges have been produced in a Mach 3 test cavity using an auxiliary discharge to stabilize the main discharge in N_2 and He/CO mixtures. A significant result is the lack of observed plasma E/N changes in response to auxiliary discharge current changes. Also, where glow discharges were obtained, the energy loading achieved was very much less than the threshold level required for laser operation.

I. INTRODUCTION

Theoretical studies (refs. 1 and 2) of the carbon monoxide electric-discharge supersonic laser show great promise for both high efficiency and power. To achieve this, however, one requires discharge methods which independently control the processes of plasma production and energy addition to the gas. The generation of a stable and spatially uniform large volume electrical discharge is an important requirement of these lasers. Direct scaling of volume, pressure, or energy input of conventional discharge schemes results in discharge instabilities, spatial nonuniformities, and eventually to a spatially localized high current arc. In principle, a desirable discharge method combines an external ionization source with a low voltage main discharge or sustainer electric field. In this way, the preionizer controls the electron density independently of the sustainer field which can be adjusted to provide the optimum electron energy for efficient vibrational excitation of neutral molecules.

Several stabilization schemes for flowing gas, electric-discharge lasers have been proposed and studied. These include the electron beam, ultraviolet flashlamp, and so-called "poker" preionization techniques. Of these, the first has been most fully exploited for use in CW laser applications. Although the electron beam technique is quite efficient and has been demonstrated to work relatively independent of gas mixtures and pressures, its

*National Research Council Postdoctoral Research Associate.

**Permanent address: Gas Dynamics Laboratory, Forrestal Campus, Princeton University, N.J., 08540.

disadvantages include: (1) the very high voltage requirements which entail extra weight to prevent arcing and to provide shielding; and (2) the current density limitations on the foils which can preclude operation at the higher desired energy loadings (refs. 2 and 3). The flashlamp approach (ref. 4) is inherently inefficient, may be less reliable, and has not been demonstrated at high energy loadings for cw applications. It does obviate the high voltage requirements of the electron beam technique. The "Poker" scheme utilizes a tailored voltage pulse train consisting of a short high voltage preionizer pulse, followed by a lower voltage, longer duration sustainer pulse. This scheme has been demonstrated for CO₂ lasers (ref. 5) and static CO laser mixtures (refs. 6 and 7), but has yet to be successfully applied to supersonic CO lasers.

Although the impetus for the study of these various discharge schemes arises from electric discharge laser technology development problems, the more general problem of stabilizing glow or large volume arc-free discharges at relatively high densities in flowing gases is also important.

The present study concentrates on addressing this important general problem of discharge stabilization in CO gas mixtures using a relatively simple discharge arrangement proposed by Blom and Hanson (ref. 8) called the Double-Discharge device. This device makes use of an auxiliary pin discharge at the cathode to provide a preionization background for stabilizing the main discharge. The technique operates in the self-sustained or avalanche mode with partial control of the ionization at the onset of the avalanche in contrast to the electron beam preionizer-sustainer configuration which totally separates the ionization and excitation processes and operates at a value of E/N well below that required for a self-sustained glow discharge.

While it is desirable to demonstrate continuous wave (cw) operating conditions, mass flow and electrical requirements dictate a more modest impulse type flow facility which provides quasi-steady flow conditions for periods of several cavity transit times (~10 msec). The experimental facilities are described in section II and the results and discussions are presented in section III followed by some concluding remarks in section IV.

We thank R. Reyes and J. Licursi for their help during the fabrication of experimental apparatus.

II. EXPERIMENTAL DETAILS

The experimental arrangement can be broadly divided into two parts: the flow facility and the electric discharge arrangement.

The flow facility, which provides a quasi-steady supersonic flow in the test channel, consists mainly of a Ludwig tube, wafer sphere butterfly valve, test channel, dump tank and a vacuum pump assembly as shown in figure 1.

A conventional Ludwig tube, 11 m long and made from 7.5 cm I.D. stainless tube with 3.8 cm wall, was used as a gas supply. A vacuum pump, pressure gauges, and a gas supply manifold were connected to the tube through pressure ports in the tube wall.

Instead of the conventional diaphragm rupture to initiate flow, the present arrangement utilizes a wafer sphere butterfly valve. The valve opens much slower than the diaphragm, but due to the large area of the valve opening and the 11 m tube length, steady flow times of greater than 10 msec could be generated for all gases tested. The principal advantages in using the valve in place of a diaphragm are: (1) the time saved by not having to change diaphragms and pumping out the driver tube and (2) avoidance of contamination of test gases by not having the tube exposed to the atmosphere between runs. The air actuated valve is activated by a solenoid valve which is controlled by a switch on the control panel. A microswitch, which senses the position of the valve handle, provides an initial pulse to trigger a series of delay circuits which control the timing of the discharges and related instrumentation.

The plexiglass channel and nozzle assembly, shown schematically in figure 2, is located just downstream of the butterfly valve. The two-dimensional contoured nozzle provides uniform supersonic flow in the test section. The nozzle used for these tests has an area ratio of 4 (Mach number, $M \sim 3$) and was designed for N_2/CO flows, including boundary-layer corrections.

The test channel is 2 cm \times 7.5 cm at the entrance and has a divergence of 0.75° on the top and bottom walls of the channel along its length to correct for the boundary-layer growth and gas heating. Each diverging wall contains a 6.5 cm \times 15 cm flush mounted copper electrode. The edges of the electrodes have a 3 mm radius which is not exposed to the flow being filled with epoxy to minimize flow disturbances.

The parallel side walls each contain two 2.5 cm \times 10 cm \times 6 mm thick calcium fluoride windows which are flush with the interior surface of the channel. The test section is connected to an 8 m³ dump tank through a 2 m long, essentially conical, transition section which expands from 10 cm I.D. from the test section exit to 20 cm I.D. at the dump tank entrance.

The electric discharge arrangement consists of two distinctly different discharge circuits. One, called the main discharge, is powered by a long-time constant capacitor discharge, and the other, called the pin discharge, is powered by a dc power supply.

A schematic of the main discharge circuit is shown in figure 3. Current is supplied to the anode from a 75 μ f capacitor bank through a current limiting, variable ballast resistor when ignition S_1 is conducting. The magnitude of the ballast resistor (278 Ω to 2500 Ω) and the capacitor charging voltage (up to 20 kV) determine the anode current level. At its minimum value the ballast provides an essentially dc current pulse with less than 10 percent decay for 2 msec (approximately ten cavity flow-transit times) at currents up to 75 amps (approximately 0.75 amps/cm² anode current density). The current

pulse is terminated by causing ignitron S_2 to conduct. The 500 k Ω resistor across the electrodes was installed for safety.

Specially designed delay and thyatron circuits initiate the main discharge at an appropriate time after steady flow is established and terminate it before the current droop becomes excessive. The times of S_1 firing after flow initiation and of S_2 firing after S_1 were recorded on separate 10 MHz counter/timers. The anode current I_a and voltage V_a are measured on an oscilloscope using a Hall effect generator and a Tektronix high voltage probe, respectively.

The second discharge called the pin discharge operates continuously. Imbedded in the cathode are 40 tungsten pins, insulated from the cathode, which form the anodes for the pin discharges. The tungsten pins (0.75 mm diam) are spaced 1 cm apart and are arranged in 10 rows (in the flow direction) of 4 pins per row (fig. 2). The pins are electrically isolated from the cathode by 1.5 mm O.D. alumina tubing. The cathode is water cooled to dissipate the heat generated by the pin discharges. The power supply for the pins can deliver a maximum current of 4 amps at 2 kV. A current limiting ballast resistor (2 k Ω - 100 W for each pin) network mounted on the side of the pin power supply distributes power to a predetermined set of pins during the experiment.

The pin current is usually determined by measuring on an oscilloscope, the voltage drop across a 10 Ω series resistance on an arbitrary pin. The total pin current from the power supply is also measured. Current measurements on a number of individual pins and the total pin current confirm that the pin-to-pin current variation is less than 10 percent.

III. RESULTS AND DISCUSSION

A. Flow Quality

In addition to measuring the pressure in the test cavity and stagnation region, a spark Schlieren was used to check the flow quality. Figure 4 shows typical pressures measured using Statham (unbonded strain gauge type) pressure transducers in the test cavity and in the stagnation region of the nozzle for nitrogen gas for an area ratio of 4 nozzle. The measured pressures imply a nominal flow Mach number of 3 in the test section for this gas. As can be seen the duration of steady flow is typically about 50 msec for N_2 , CO, or argon gas and about 15 msec for helium gas. These pressure traces indicate that the butterfly valve takes about 10-15 msec to establish a steady flow in the channel and that the head of the expansion wave arrives at the nozzle throat at about 75 msec after initiating the valve opening in nitrogen gas.

The variation of the pressure in the test channel over this 50 msec duration is always less than 5 percent of its nominal value. Since the (electric) discharge pulse duration is always less than or equal to 4 msec, the variation

in the pressure during this test period is really negligible. This observation is true for all the gases used in the present investigation.

A spark Schlieren with 7.5-cm field of view and about 3 μ sec spark duration was set up to examine the flow quality in the test channel. Figure 5 shows typical Schlieren pictures for a nitrogen flow. The location of the leading and trailing edges of the electrodes are denoted in figure 5. (Note: The distance between the leading and trailing edges (15 cm) is not shown to scale in fig. 5.) The cavity pressure measured 2.5 cm upstream of the electrodes and the corresponding stagnation pressure are also shown in figure 5. The two Schlieren pictures are from separate runs with identical conditions. The waves emanating from the leading and trailing edges of the electrodes are Mach waves, that is, the angles made by these waves with the flow direction corresponds to the local Mach angle. The epoxy which has been used to make up the gap between the rounded electrodes and the channel walls seems to be responsible for these weak disturbances. The boundary layer on the walls of the channel appears to be thin, typically less than 3 mm at this pressure.

B. Pin Discharges

In a typical experimental situation a predetermined set of pins are used for the auxiliary discharge. The pin discharges are initiated before a run using a subsonic N_2 or He flow. The subsonic flow of bleed gas is turned off just before run initiation. Thus, the pins are arcing continuously through flow initiation until after the flow ceases.

The detailed structure of these auxiliary pin discharges is not known, due to their very small size and the relatively short time duration of the main discharge. However, certain gross features were observed. A pin potential of approximately 350 V is required before any significant current is drawn. Further increases in pin current up to the maximum of 200 mA/pin are accomplished with relatively small voltage changes. The maximum pin current limitation is dictated by the wattage of the individual pin ballast resistors and/or the 4 amp maximum current available from the power supply.

As pin current is increased during the subsonic flow portion of run preparation, with both main electrodes grounded, the discharge region is observed to increase as sketched in figure 6. The thickness of these discharges normal to the cathode is less than 2 mm. The behavior during supersonic flow is somewhat different. The luminous regions extend downstream to the cathode trailing edge and their thickness normal to the cathode decreases. Correspondingly, the pin current decreases from its value set during the subsonic flow. The oscilloscope traces of pin current show that it achieves a steady-state value before the main discharge is initiated. The reduced pin current under supersonic flow is consistent with the increased number density and pin discharge area observed.

C. Voltage-Current Characteristics at Low Main Discharge Current

$$(I_a \leq 1 \text{ amp})$$

This section describes the voltage-current characteristics in N_2 , N_2/CO , He/CO , and Ar/CO gas; and gas mixtures under the condition where the magnitudes of the main and auxiliary discharge currents are comparable (~ 1 amp).

Figure 7 shows typical oscilloscope traces of voltage-current characteristics from tests using commercial grade nitrogen gas in a Mach 3 flow at a cavity pressure of 12 torr. The discharge duration of 4 msec used here corresponds to about 20 gas flow exchange times across the 15 cm long electrodes. The four pictures correspond to four different experiments done under identical conditions except for varying total pin current. Fourteen pins, composed of the two nearest the cathode centerline in the first seven rows, were used. (It appears from a large number of tests that pin geometry does not play a dominant role in the basic discharge behavior.)

The voltage-current time histories of figure 7 show a glow discharge type behavior in which both the voltage and current remain constant during the test period after the discharge initiation transient. (The rise in anode current at discharge termination arises from the fact that the plasma impedance is much larger than that of the ignitron S_2 when it is conducting.) The most significant feature of figure 7 is that the main discharge voltage and current are essentially independent of pin current variations. (This point will be addressed in more detail below in connection with fig. 10.)

Another series of results for fixed pin current and geometry for a variety of cavity pressures in pure nitrogen are shown in figure 8. The important feature of these current-voltage characteristics is that the main discharge voltage scales linearly with pressure if one subtracts the 350 V pin voltage from the anode voltage. Also, there appears to be less stable behavior, especially at discharge initiation, as cavity pressure is increased. Stable discharges have been observed in pure nitrogen up to cavity pressures of 50 torr. However, at higher pressures a steady arc persisted for the duration of the discharge.

The importance of at least some small auxiliary pin discharge current is shown in figure 9. In the absence of pin discharges, an arc is formed within a few microseconds of the discharge initiation and this corresponds to the anode voltage dropping to zero in figure 9(b). This is also seen in figure 9(d) followed by oscillations in the voltage and current traces. The spikes in figure 9(d) correspond to the arcs which are repetitively formed; the arc, after its formation each time, is swept off the electrodes with the local flow velocity. The time interval between successive spikes here correspond approximately to one cavity transit time for the flow. Confirmation of this behavior has been recently reported by Garcia et al. (ref. 9) from tests under similar conditions in which arc velocity was measured using a pair of photomultiplier tubes each with a small aperture spaced a known distance apart. Measuring the time intervals between light pulses which were associated with individual arcs, they showed that the arcs were swept downstream at

the flow velocity. Figures 9(a) and (c) show that in the presence of pin discharges the voltage and current traces show a glow discharge type of behavior indicating that pin discharge is, indeed, necessary to have a stable glow discharge.

One of the crucial questions considered in the present investigation is whether the auxiliary pin discharges provide independent control of plasma E/N, the ratio of the electric field to the total number density. Blom and Hanson (ref. 8) suggested that this was indeed a possibility based on a comparison of results obtained in a supersonic nitrogen flow with a variety of very small auxiliary discharge currents. However, as the main discharge current increased, their E/N values approached a constant limit of approximately 2×10^{-16} V-cm². This is similar to the behavior exhibited in figures 7 and 8.

A conclusive demonstration of the fact that auxiliary pin discharge current variations have little influence on main discharge E/N in these single electrode tests is presented in figure 10. This summarizes the behavior of E/N as a function of total pin current in a variety of test gases at a variety of cavity pressures in which stable, relatively low current, volume discharges were observed. The electric field E is calculated by subtracting the pin voltage of 350 V from the anode voltage and dividing the result by the average electrode separation, 2.5 cm. The total number density is used to compute E/N in each case. It is clear that test gas composition is much more important than auxiliary pin discharge current in determining plasma E/N except for the case of very low pin currents.

These values of E/N (2 to 4×10^{-16} V-cm²) are higher than the optimum required ($\sim 1 \times 10^{-16}$ V-cm²) for efficient vibrational excitation of the diatomic molecule. Moreover, the maximum achievable discharge current without arcing was less than 1 amp corresponding to an energy loading of at most a few hundredths of an electron volt per CO molecule in those mixtures containing 5 percent molar fractions of CO. This energy loading is approximately an order of magnitude below that required for threshold lasing.

Initial attempts to add small concentrations of CO to N₂ and He carrier gases were not successful insofar as a stable discharge is concerned, even at these low current density conditions. Addition of CO to N₂ increased the E/N (fig. 10) and tended to destabilize the discharge. The voltage-current characteristics for discharges in CO dilute mixtures in N₂ and He are shown in figure 11. The cavity pressures, pin geometry, and total pin current are similar to those used in the pure N₂ discharges (figs. 7 and 8). However, the behavior is quite different, resembling that shown in figure 9; the oscillatory behavior depicted in the voltage-current traces in figures 11(a) and (b) correspond to the formation of arcs at or near the leading edge of electrodes which are swept downstream. The time interval between two voltage spikes is about 250 μsec for the N₂/CO mixture and about 100 μsec for the He/CO mixture; this time corresponds to the passage of one slug of gas across the 15-cm-long electrode with N₂/CO and He/CO gas mixture, respectively. The gases used in all these experiments (figs. 5 through 11) is of commercial purity grade. Furthermore, the CO passed through a room temperature activated carbon filter before entering the driver tube.

When a premixed gas mixture of research grade CO in He, also of high purity grade, was used as a test gas, completely stable glow discharges were achieved in both 5 and 10 percent CO in helium diluent and up to a pressure of 20 torr in a Mach 3.5 supersonic flow. The voltage-current oscilloscope traces for these cases is shown in figures 12 and 13. As seen in figure 12(b), for CO concentration more than 10 percent in He, the discharge has a tendency toward arcing. Also, for cavity pressures exceeding 20 torr, there is a similar tendency as exhibited in figure 13(b). The absence of stable glow discharges in the commercially pure grade gas mixtures may be due to the presence of some impurities which have a destabilizing effect on the discharge.

In all these experiments, the pins do not seem to have any effect in varying E/N. The values of E/N for these mixtures are essentially constant for pin current variations of a factor of 5 as shown in figure 10. There appears to be a slight dependence on density with E/N decreasing as density is increased, particularly for the helium mixture. For example, 5/95 percent CO/He mixture at 10 to 20 torr has an E/N of $\approx 1 \times 10^{-16}$ V-cm², but its value at 5 torr is at least 50 percent larger. Similar behavior is also observed for 10 percent in He. The reason for this different behavior at this low pressure is not clear. At these low pressures, the boundary layers on the walls are very diffuse, and what role these thick boundary layers might play in controlling the plasma characteristics is not known.

For the mixture of 10 percent CO in He, the E/N values are higher compared to 5 percent CO in He. This is expected because of the higher CO concentration in these mixtures.

The value of E/N of 1 to 2×10^{-16} V-cm² for these mixtures in the present experiments is still high for most efficient vibrational excitation of CO. The typical energy loading of ≤ 0.03 eV/diatomic molecule achieved in these low current operation experiments is well below the threshold energy loading for laser operation. In this sense, the present scheme of discharge stabilization is not practical for a laser device. Although the presence of pin discharges is shown to stabilize a volume discharge over a limited range of experimental parameters, the facts that the plasma E/N cannot be independently controlled by varying pin discharge characteristics and that the main discharge currents are limited to an amp or less means that this conceptually simple, single electrode scheme is not very useful for CO electric discharge lasers.

D. Voltage-Current Characteristics at Large Main Discharge Current ($I_a > 1$ amp)

For a given test condition, the current in the main discharge circuit can be increased by either decreasing the current limiting ballast resistor (fig. 3) or by increasing the capacitor bank charging voltage. The former method is preferred since for a given discharge current the initial voltage on the gap before breakdown is lower. Both approaches were employed and led to essentially the behavior described below.

It is observed that whenever the main discharge current exceeds 1 amp, the discharge is no longer stable and immediately goes into an arcing mode similar to that seen in figure 11. For main discharge currents greater than 10 amps, a steady arc is observed at the trailing edge of the electrodes. Figure 14(a) exhibits, through a series of photographs taken with 1 μ sec exposure time using a Beckman-Whitley image converter camera, that this steady arc moves with the flow at the local flow velocity. The field of view of the camera in these pictures is so arranged that the trailing edge of the 15-cm-long electrodes is located near the left edge of these pictures. The times t indicated below these photographs correspond to the time elapsed since the initiation of the main discharge. The four time resolved photographs shown here are taken from four different experiments performed under identical conditions.

Typical voltage-current oscilloscope traces are also shown in figures 14(b) and (c). The arc formation is very rapid. The sweep speed in figure 14(b) is too slow to resolve the initial voltage spike, but this is shown more clearly in figure 14(c) where it is observed that the initial breakdown occurs during the first microsecond. Note the difference in voltage and time scales between figures 14(b) and (c). Also, the discharge duration for the particular test shown in figure 14(c) was only 600 μ sec versus the 4 msec time in figure 14(b). The relatively slow rise in voltage after breakdown, observed during the first 500 μ sec of figure 14(b), is attributed to the fact that the arc is being "blown" downstream with an ever lengthening discharge path. After the arc extends downstream some 10 to 20 cm, it appears to achieve some quasi-steady configuration with a corresponding relatively constant voltage, that is, the arc continues to conduct with moderate (<30 percent) voltage fluctuations. Two possible reasons why the arc achieves this quasi-steady state at this location are: (1) the boundary layers merge at this point, or (2) this location corresponds approximately to the end of the test section with a subsequent sharp area increase.

Although the results shown in figure 14 are for CO/Ar mixture, similar behavior has been observed in all gases and gas mixtures studied at these discharge conditions.

Since switching the high voltage to the anode from the capacitor bank is done through an ignitron switch, coupling of high voltage is not gradual but is instantaneous (but for a small circuit inductance). Although the current in the circuit is limited by the ballast resistance, this particular switching method of high voltage causes avalanche mode operation for all capacitor charge voltages exceeding that established by the glow discharge. This method of main discharge initiation was suspected of playing an important role in the establishment of the quasi-steady arc phenomena exhibited in figure 14. That is, in those tests the entire capacitor bank charging voltage was applied to the anode within 1 μ sec before the main discharge began to conduct. Therefore, a small 0.1 μ f capacitor was connected between the anode and cathode. This extended the rise time of the initial voltage pulse from fractions of a microsecond to values between 27 and 250 μ sec depending on the ballast resistor employed. The current-voltage characteristics for some tests in CO-Ar mixtures, which are typical of the behavior observed in all test gases, are

shown in figure 15. Figure 15(a) can be compared with figures 14(b,c). Taking the different sweep speeds and voltage sensitivities into account, these two results are essentially the same, that is, even with relatively slow discharge initiation, high current density operation produces a large quasi-steady arc which extends downstream from the electrode trailing edges.

Low current discharges (~ 2 amps) are shown for comparison in figure 15(b) (without capacitive loading of the electrodes) and figure 15(c) (with capacitive loading). The behavior is similar for both cases in that successive arcs are formed, each taking the better part of one cavity transit time to be swept off the electrodes. That is, insufficient current density exists to provide a quasi-steady arc. The major differences between these two cases are that with capacitive loading a voltage of approximately 3 kV is required to form the arc versus approximately 2 kV without capacitive loading. Also, from figure 15(c), essentially no current is drawn during the voltage buildup phase of the cycle and during each arc the voltage drops to a very low value as compared to the noncapacitively loaded case.

These results provide more evidence for the conclusion that the auxiliary pin discharges are not capable of stabilizing discharges at the current densities required for laser operation.

IV. CONCLUDING REMARKS

Stable, volume glow discharges have been obtained in supersonic N_2 , N_2/CO , and He/CO flows at cavity pressures up to 50 torr for the former and 20 torr for the latter mixtures. The energy loadings achieved were very small, of the order of 0.03 eV/diatomic molecule, and not of practical interest for lasers. Attempts to increase the energy loading were unsuccessful in that arcing dominated the discharges.

The auxiliary pin discharge, used to provide a preionization background for the main discharge, is capable of stabilizing a volume discharge only over a very limited range of main discharge current densities. Furthermore, no evidence exists that the auxiliary pin discharge is capable of providing independent control of plasma E/N. The values of E/N, observed when volume discharges existed, were too high for most efficient vibrational excitation of CO.

The addition of small amounts of CO (5 to 10 percent) had the effect of destabilizing the discharge and significantly raised the plasma E/N. Therefore, it is unlikely that this single anode configuration is a concept that has practical application to CO electric discharge lasers.

V. REFERENCES

1. Monson, D. J.: Potential Efficiencies of Open- and Closed-Cycle CO, Supersonic, Electric-Discharge Lasers. AIAA Journal, vol. 14, no. 5, May 1976, pp. 614-620.
2. Mann, M. M.: CO Electric Discharge Lasers. AIAA Journal, vol. 14, no. 5, May 1976, pp. 549-567.
3. Jones, T. G.; Byron, S. R.; Hoffman, A. L.; O'Brien, B. B.; and Lacina, W. B.: Electron-Beam Stabilized CW Electric Discharge Laser in Supersonically Cooled CO/N₂/Ar Mixtures. AIAA Paper 74-562, presented at the AIAA 7th Fluid and Plasma Dynamics Conference, Palo Alto, California, June 1974.
4. Lind, R. C.; Wada, J. Y.; Dunning, G. J.; and Clark, W. M., Jr.: A Long-Pulse High Energy CO₂ Laser Pumped by an Ultraviolet-Sustained Electric Discharge. IEEE Journal of Quantum Electronics, vol. QE-10, no. 10, Oct. 1974, pp. 818-821.
5. Hill, A. E.: Continuous Uniform Excitation of Medium Pressure CO₂ Laser Plasmas by Means of Controlled Avalanche Ionization. Applied Physics Letters, vol. 22, no. 12, June 15, 1973, pp. 670-673.
6. Monson, D. J. and Lee, C. M.: Pulsar-Sustainer Glow Discharge Operation in Static Carbon Monoxide Laser Mixtures. Paper presented at the Conference on Partially Ionized Plasmas, Princeton University, Princeton, N. J., June 10-12, 1976.
7. Hill, A. E. and Moeny, W. M.: Cryogenic "Poker" CO Electric Laser. 29th Annual Gaseous Electronics Conference, Oct. 1976.
8. Blom, J. H. and Hanson, R. K.: Double-Discharge Arrangement for CW Electrical Excitation of Supersonic Flows. Applied Physics Letters, vol. 26, no. 4, Feb. 15, 1975, pp. 190-192.
9. Garcia, M.; Bienkowski, R.; and Lawless, J.: Stabilization of a Supersonic Flow Gas Discharge by Auxiliary Pin Discharges. 29th Annual Gaseous Electronics Conference, Oct. 1976, to be published in Bull. Am. Phys. Soc.

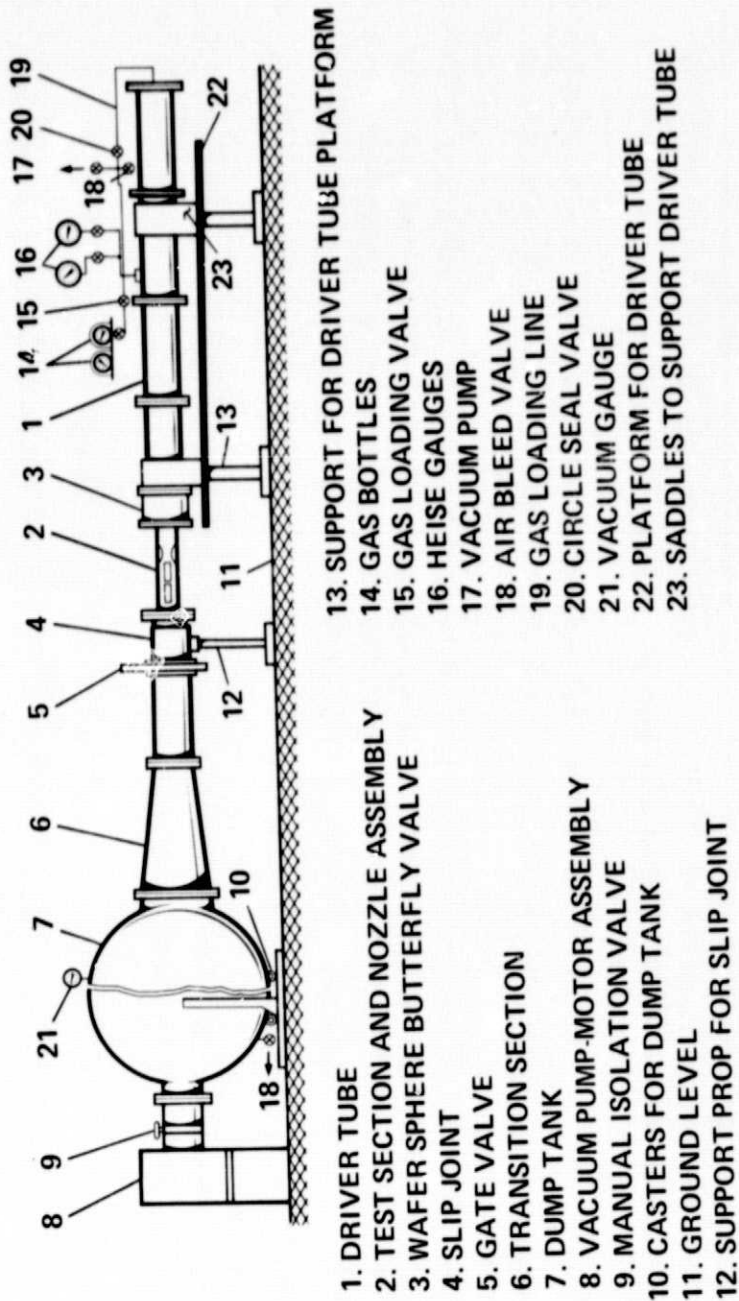


Figure 1.- Schematic of the supersonic flow double discharge facility.

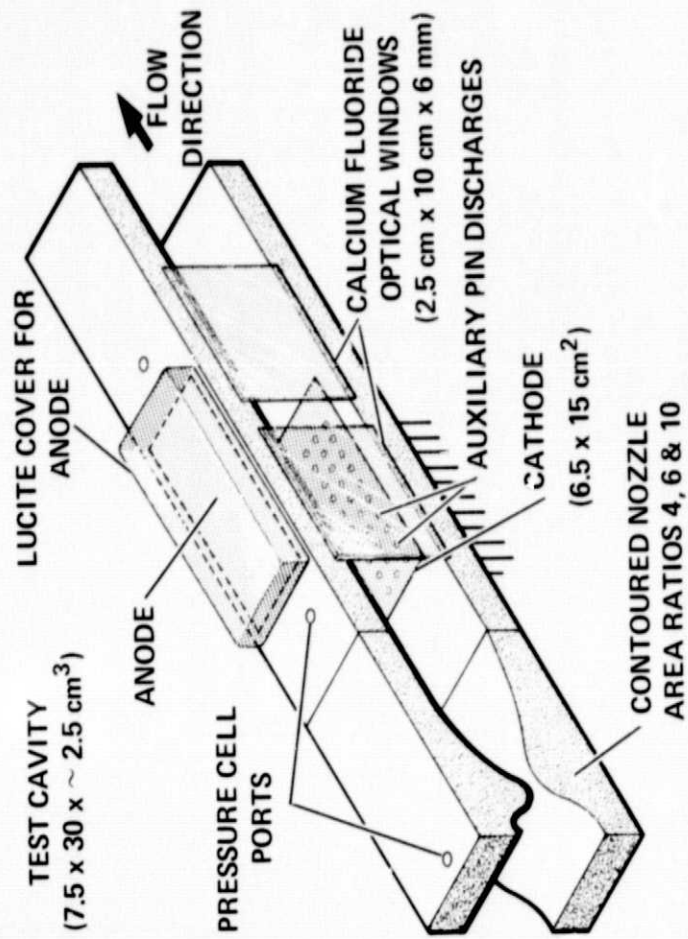


Figure 2.- Nozzle and test section assembly.

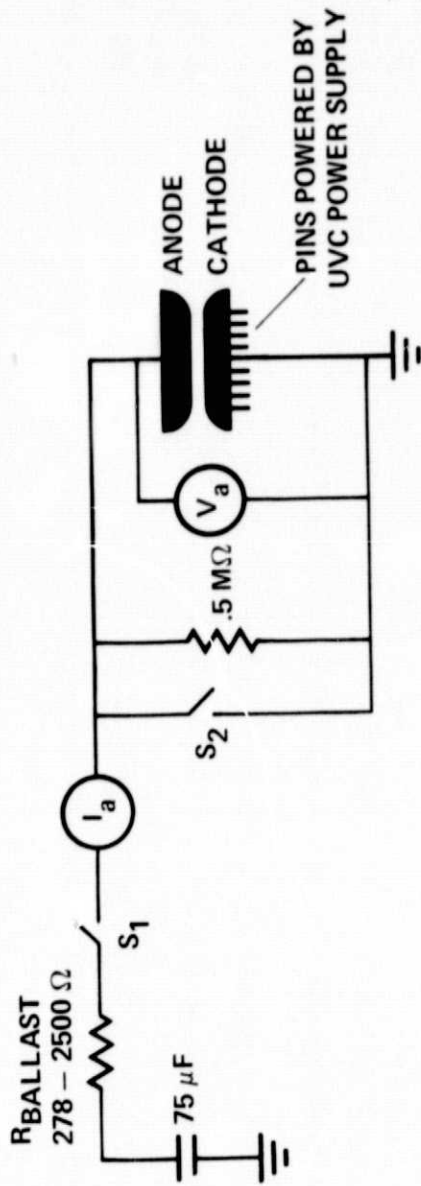
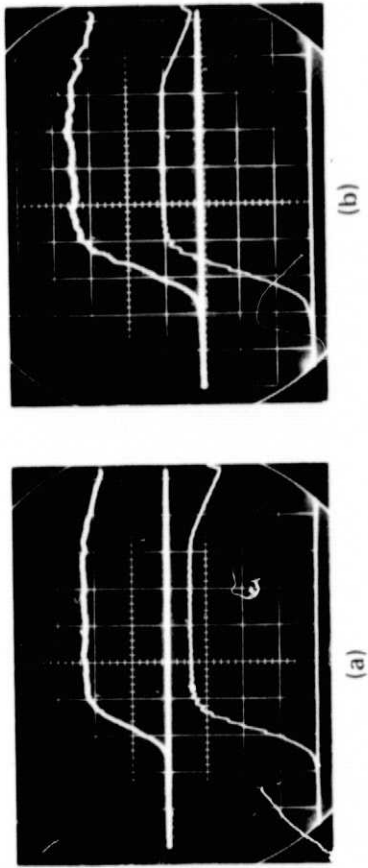
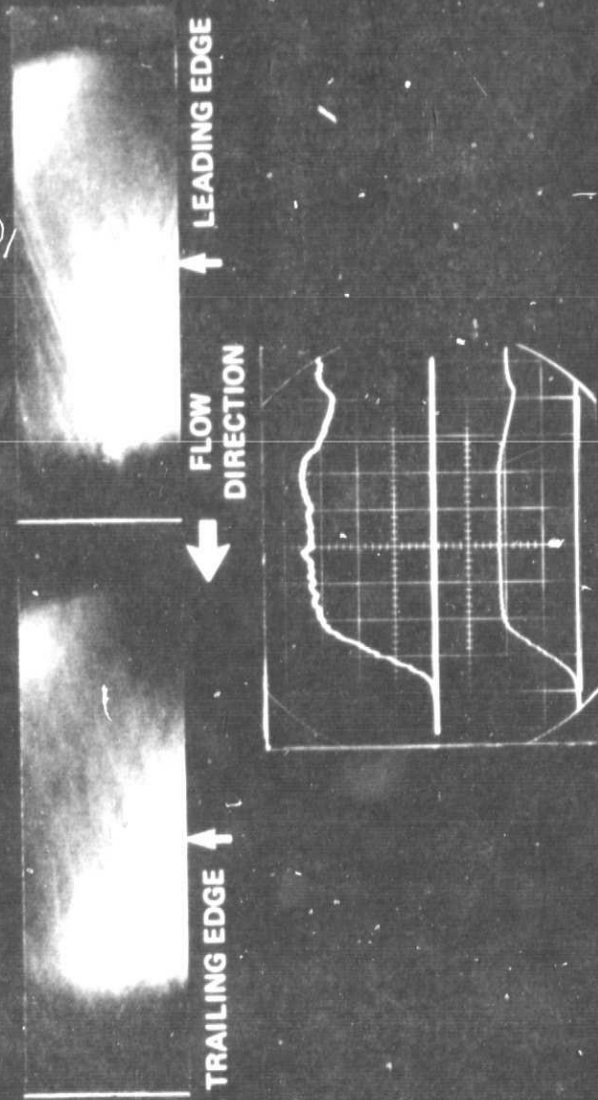


Figure 3.- Schematic of the electric discharge circuit.



UPPER TRACE: STATIC PRESSURE: (a) 10.5 Torr/div. (b) 21 Torr/div.
 (CAVITY PRESSURE, P_C)
 LOWER TRACE: STAGNATION PRESSURE: (a) 5 psi/div. (b) 12.5 psi/div.
 SWEEP: 10 msec/div. FOR (a) AND (b)
 INITIAL DRIVER PRESSURE AND GAS: (a) 20 psi N₂ (b) 50 psi N₂

Figure 4.- Typical static and stagnation pressure oscilloscope records.



UPPER TRACE: P_C : 21 Torr/div.

LOWER TRACE: STAG: 1400 Torr/div.

SWEEP SPEED: 10 msec/div.

INITIAL DRIVER TUBE PRESSURE = 60 psi N_2

Figure 5.- Typical Schlieren pictures show the flow quality in the test channel.

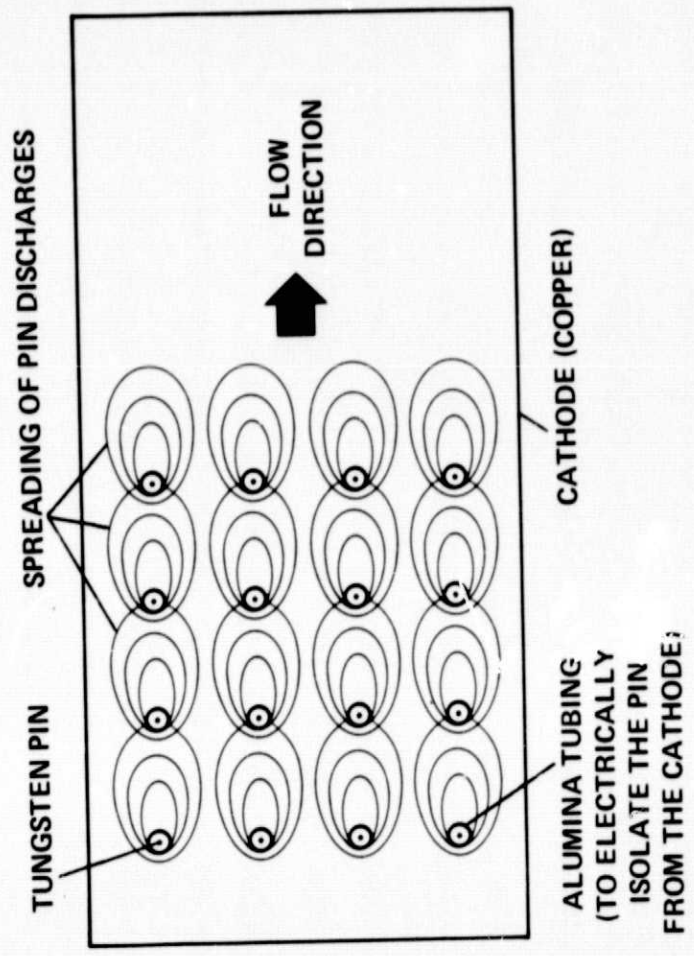
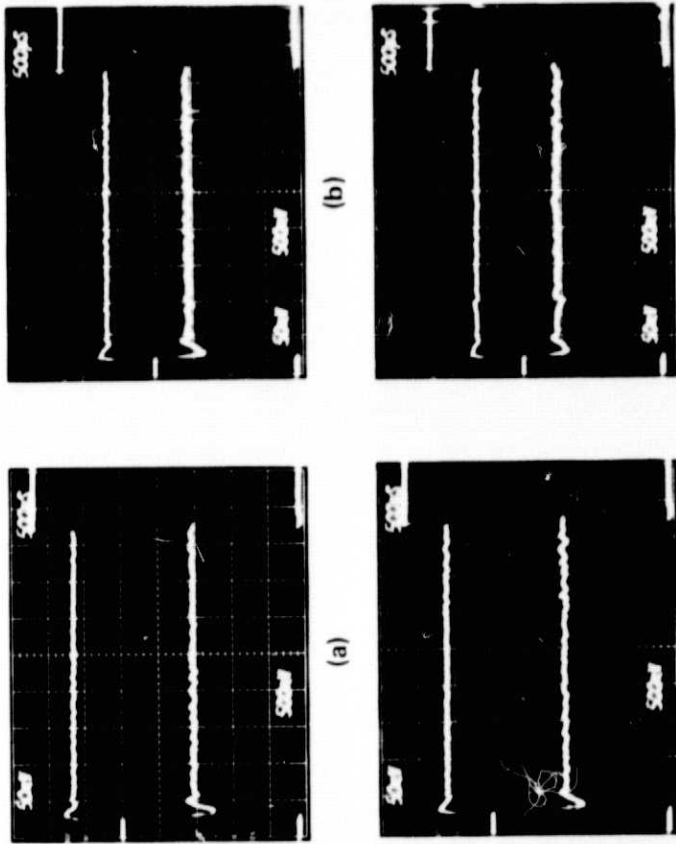


Figure 6.- Pin discharges with the flow.



(a) (b) (c) (d)

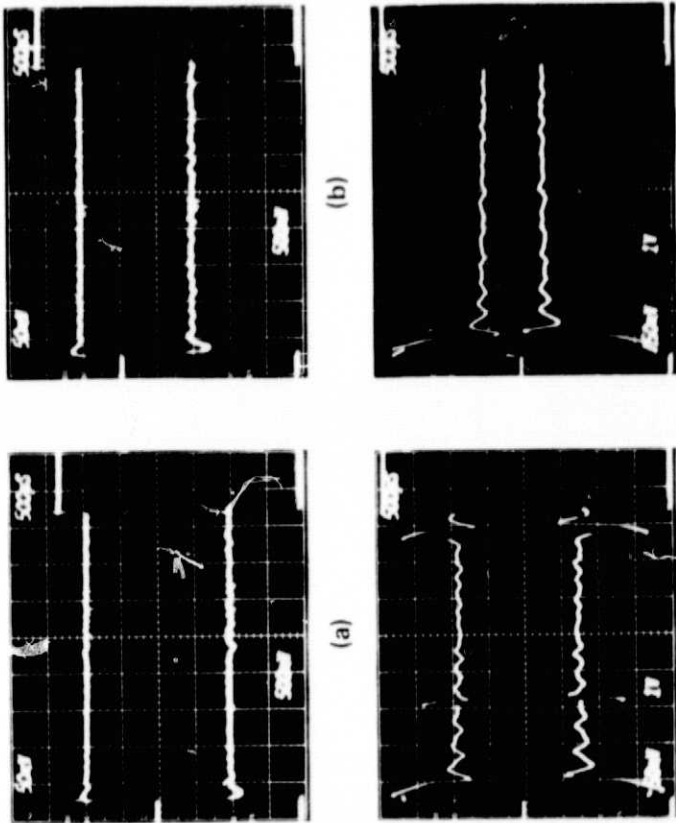
12 Torr Ni_2 , $M = 3.0$, 14 PINS, $V_{\text{CAP}} = 3.0 \text{ kV}$

UPPER TRACE: $I_a = 0.5 \text{ A/div.}$ LOWER TRACE: $V_a = 500 \text{ V/div.}$, SWEEP SPEED: $500 \mu\text{sec/div.}$

(a) $I_{\text{PINS}} = 0.95 \text{ A}$ (b) 2.0 A (c) 2.25 A (d) 2.5 A

$E/n \cong 4 \times 10^{-16} \text{ Volt-cm}^2 \text{ FOR ALL CASES}$

Figure 7.- Effects of varying pin current on discharge characteristics.



(a)

(b)

(c)

(d)

NITROGEN; $T_{\text{CAV}} \cong 100^\circ \text{K}$; $M = 3$, 14 PINS , $I_{\text{PINS}} = 2.5 \text{A}$

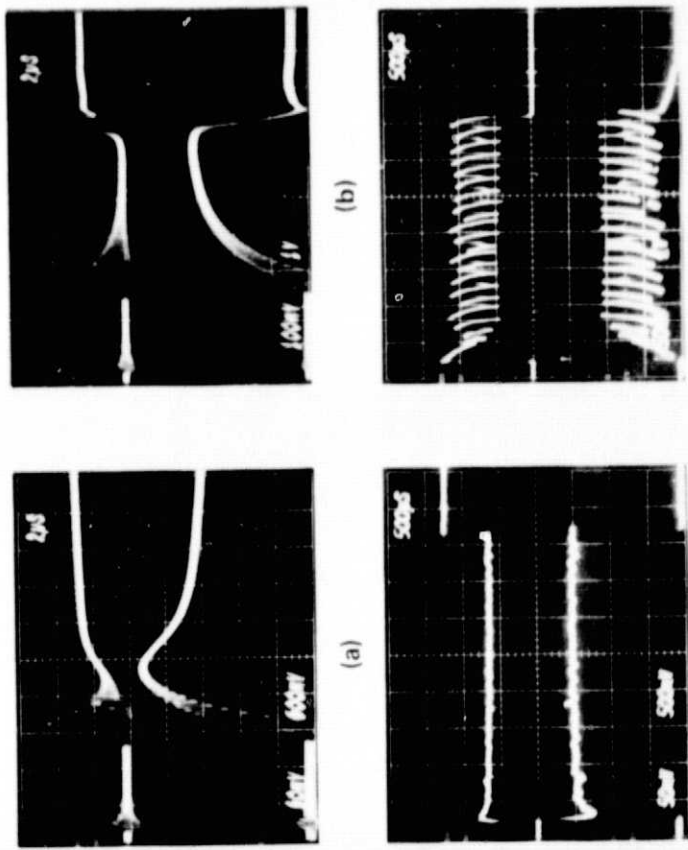
UPPER TRACE: I_a : 0.5A/div . LOWER TRACE: V_a : 0.5kV/div . (a) and (b), 1.0kV/div . (c) and (d)

SWEEP SPEED: $500 \mu\text{sec/div}$.

CAVITY PRESSURE, P_C : (a) 6 Torr, (b) 12 Torr, (c) 24 Torr, (d) 36 Torr

$E/n \cong 4 \times 10^{-16} \text{ Volt-cm}^2 \text{ FOR ALL CASES}$

Figure 8.- Effect of cavity density on discharge characteristics in nitrogen gas.



WITH PIN DISCHARGE WITHOUT PIN DISCHARGE
 12 Torr NITROGEN, $V_{CAP} = 3.0$ kV, $M = 3.0$
 I_a: UPPER TRACE/div 0.5A 1.0A 0.5A 0.5A
 V_a: LOWER TRACE/div 0.5 kV 1.0 kV 0.5 kV 1.0 kV
 SWEEP SPEED/div 2 μsec 2 μsec 500 μsec 500 μsec

Figure 9.- Comparison of discharge behavior with and without auxiliary pin discharges.

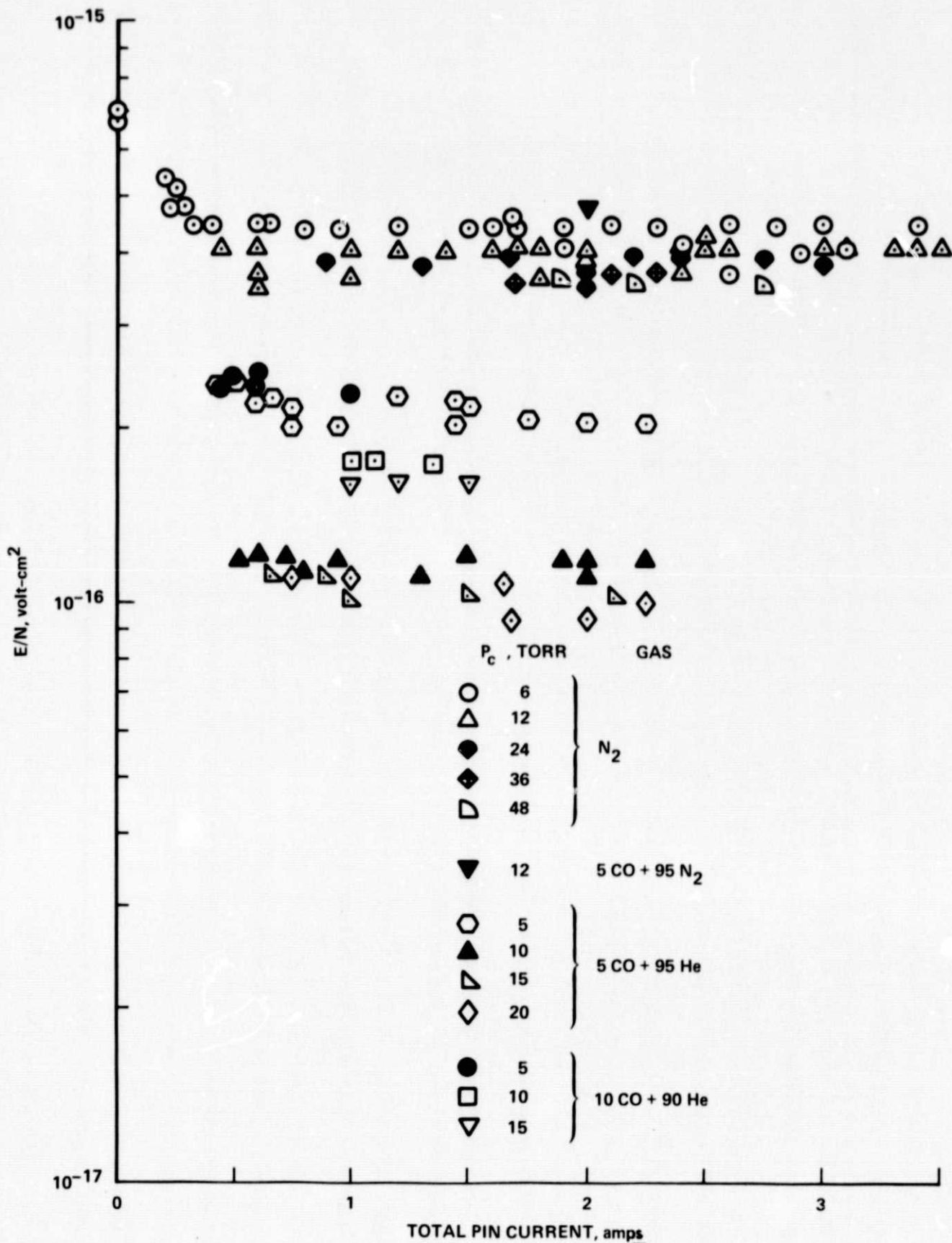
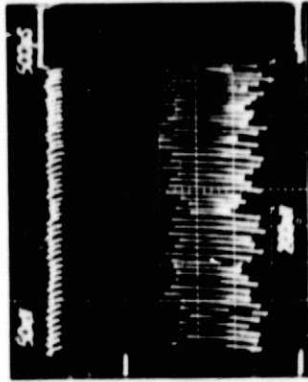


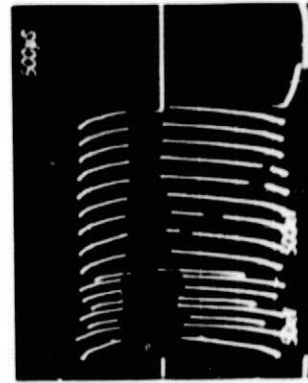
Figure 10.- Plot of E/N as a function of total pin current for different gases.



(a)

UPPER TRACE: I_a : 0.5A/div.

LOWER TRACE: V_a : 500V/div. FOR (a)
and V_a : 200V/div. FOR (b)



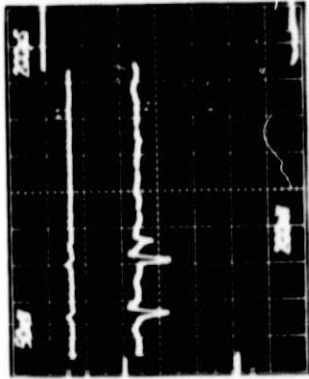
(b)

SWEEP SPEED: 500 μ sec/div.

CAVITY PRESSURE, $P_C = 12$ Torr, 14 PINS, $I_{PINS} = 2.5$ A, $V_{CAP} = 3.0$ kV

(a) 0.02 CO + 0.98 N₂ (b) 0.02 CO + 0.98 He

Figure 11.- Effect of impure CO addition to nitrogen and helium.



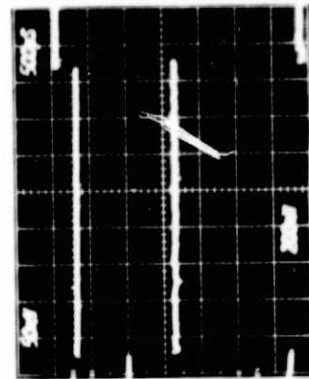
(a)

UPPER TRACE: I_a : 0.5A/div.

LOWER TRACE: V_a : 200 V/div.

SWEEP: (a) 500 μ sec/div., (b) 200 μ sec/div.

CAVITY PRESSURE = 10 Torr at $\sim 75^\circ$ K



(b)

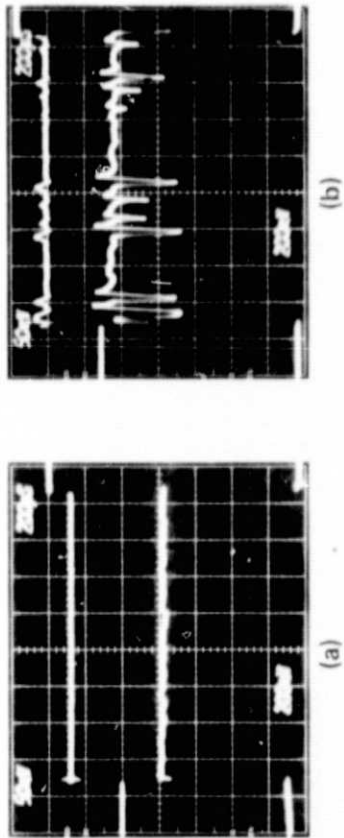
a) 5% CO + 95% He

TOTAL PIN CURRENT = 0.95A

b) 10% CO + 90% He

TOTAL PIN CURRENT = 1.3A

Figure 12. - Glow discharges in high purity CO + He mixtures.



UPPER TRACE: I_a : 0.5 A/div.

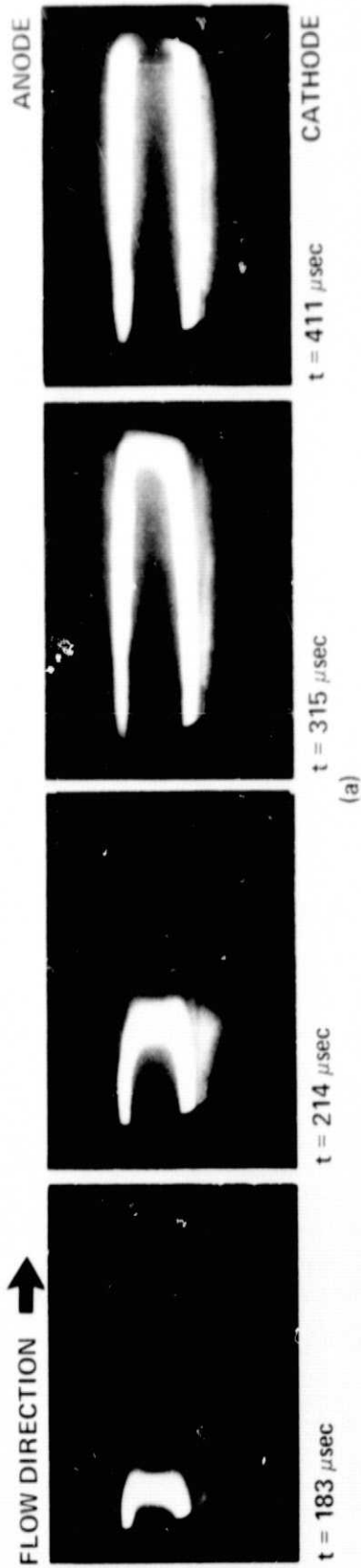
LOWER TRACE: V_a : 200V/div.

SWEEP: 200 μ sec/div.

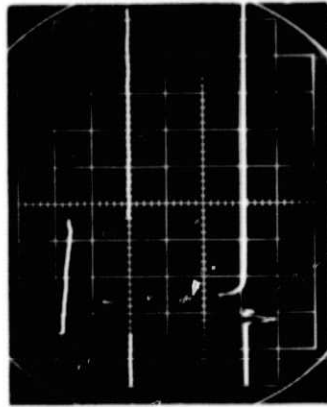
$T_{\text{cavity}} \sim 75^\circ \text{K}$, P_C : (a) 10 Torr, (b) 20 Torr

TOTAL PIN CURRENT $\approx 2A$

Figure 13.- Effect of cavity density on discharge characteristics in 0.05 CO + 0.95 He mixtures.



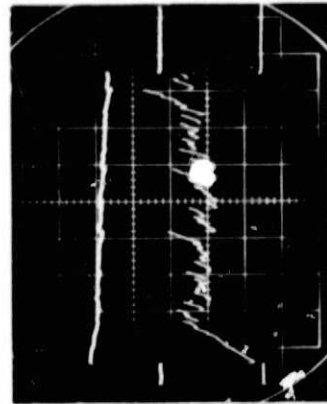
(a)



UPPER TRACE: I_a : 20A/div.,
SWEEP: 200 $\mu\text{sec}/\text{div}$.

LOWER TRACE: V_a : 2kV/div.,
SWEEP: 2 $\mu\text{sec}/\text{div}$.

(c)



UPPER TRACE: I_a : 20A/div.

LOWER TRACE: V_a : 0.5kV/div.

SWEEP SPEED: 500 $\mu\text{sec}/\text{div}$.

(b)

CO/Ar: 0.30/0.70, P_C : 40 Torr, NO PINS

$V_{CAP} = 10\text{kV}$, 278 Ω BALLAST, 3 cm ELECTRODES

Figure 14.- Discharge characteristics at large main discharge currents.

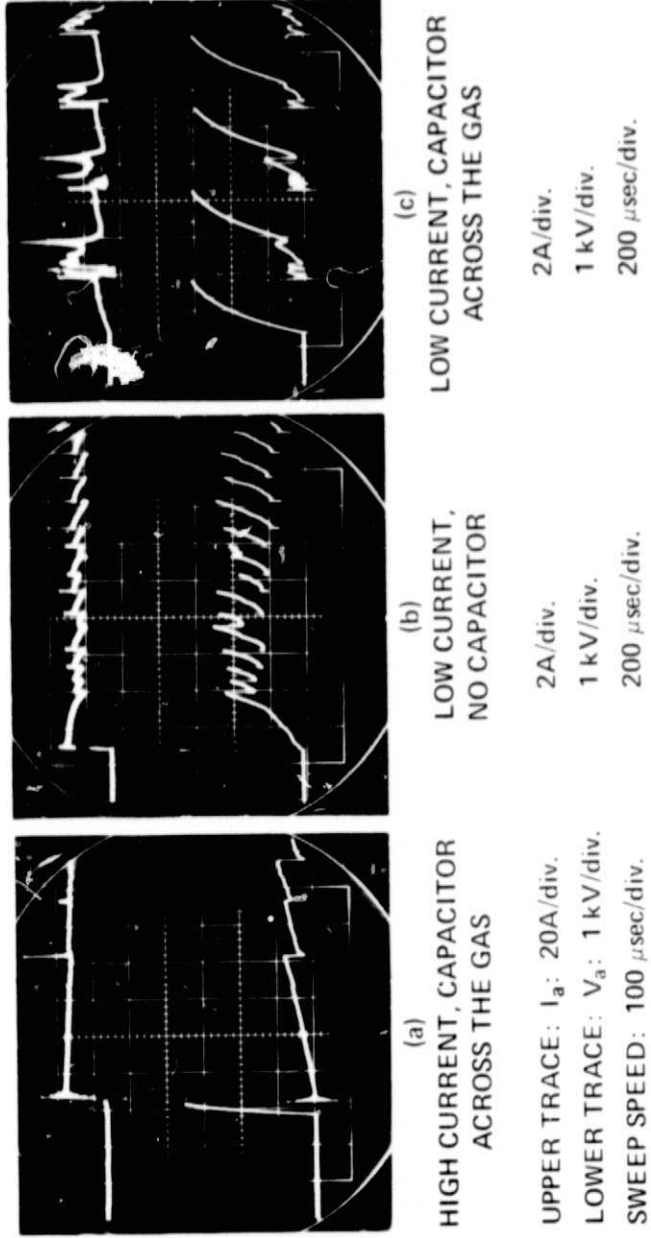


Figure 15.- Leading-edge modification of voltage pulse with a capacitor.